

RESEARCH ARTICLE

FUZZY LOGIC BASED DYNAMIC BRAKING SCHEME FOR STABILIZATION OF INTER-AREA OSCILLATIONS

M. Fayez^{1*}, M. Mandor², M. El-Hadidy³ and F. Bendary²¹Cairo Electricity Production Company Cairo, EGYPT, 22 shanan St., B.O. Box 11569²Electrical Power and Machines Department, Faculty of Engineering (Shoubra), Benha University Cairo, EGYPT, 108 Shoubra St., B.O. Box 11241³Egyptian Electricity Holding Company Cairo, Egypt, Emtedad Ramsis St., B.O. Box 11569*Corresponding Author Email: eng_mf69@yahoo.com

This is an open access article distributed under the Creative Commons Attribution License, which permits unrestricted use, distribution, and reproduction in any medium, provided the original work is properly cited

ARTICLE DETAILS

ABSTRACT

Article History:

Received 01 May 2019

Accepted 11 June 2019

Available online 13 June 2019

Power system oscillations have been long recognized as a problem of great interest in the electric power industry. The main objective of this work focuses on stabilization of inter-area power oscillations motivated by the fact that many catastrophic blackout events with the consequent multi-billion-dollar economic losses were due to the presence of unstable inter-area modes of oscillations. This study will explore dual fuzzy logic controllers to orchestrate a coordinated switching strategy for dual dynamic braking resistors, as a cost-effective method, for stabilization of inter-area power oscillations in Kundur's two-area test system. Comparative simulation study via MATLAB/Simulink-based modeling and simulation environment of the test model with and without the suggested stabilization regime will demonstrate its effectiveness in stabilizing inter-area oscillations.

KEYWORDS

Dynamic Braking Resistor, Fuzzy Logic Controller, Inter-Area Power Oscillations, Kundur's Two-Area Test System

1. INTRODUCTION

Electric power systems normally experience the oscillatory behavior in all over the world [1]. Originally, electromechanical power system oscillations were experienced as soon as the utility-scale synchronous generators were interconnected to provide more electric power supplying capabilities and more system security which means that oscillation phenomenon is inherent property in electrical power systems. Electromechanical power system oscillations can be categorized by their interaction characteristics as torsional modes of oscillations, control modes of oscillations, local plant (inter-plant) modes of oscillations, and inter-area modes of oscillations. Though all of these categories are very much related and could be very likely to manifest at the same time in the same electric power system, this work's main concentration is on inter-area oscillations.

Among the currently imaginable categories of power system oscillations, inter-area oscillations are, by far, the most destructive to the synchronous integrity of the interconnected power systems due to their wide frequency range and the huge numbers of the involved generators besides inherent weak damping associated with the inter-area oscillations which leave open wide possibilities for irrevocable blackouts with the resultant devastating consequences measured in terms of massive economic losses and possible human casualties [2,3]. In fact, many catastrophic blackout events with the consequent multi-billion-dollar economic losses were due to the presence of unstable (i.e. negatively damped) inter-area modes of oscillations. For instance, the Western Electricity Coordinating Council (WECC) blackout event that occurred on 10th of August 1996 was due to unstable inter-area oscillation mode. This memorable catastrophic blackout event was responsible for disconnecting of 28 GW electrical load and cutting off the power from nearly 7.5 million consumers with other devastating outcomes in all over the Pacific Coast of Canada and the United States. Therefore, the main objective of this work focuses on stabilization of inter-area power oscillations.

Inter-area modes, simply inter-area, oscillations are associated with combination of closely coupled generators in a power system swinging with respect to another combination of closely coupled generators in another power system. These oscillations make the two systems to experience power swings in a periodic manner with typical frequency range of 0.05 – 0.8 Hz. The damping feature of this mode is deteriorated by interconnecting two or more sub-networks via weak transmission links, the extensive utilization of the fast-acting high-gain Automatic Voltage Regulators (AVRs) and transferring bulk power transactions over long-distance transmission lines [4,5].

For predetermining the amount of power transactions through a transmission line, there has been persistent commercial stress imposed on the transmission system operators to utilize the maximum allowable power transfer limit of a transmission line due to the lack of transmission expansion projects. Moreover, due to the ongoing transition of the power industry to a deregulated platform, many transmission lines are suddenly compelled to convey heavier power transactions which incontrovertibly will provoke the inception of unstable inter-area power oscillations with the consequent increased probability of system break-ups [6,7]. Also, the increased and persistent pace of the synchronous electrical interconnection of many regional power systems all over the world results in the uprising of unstable low-frequency inter-area oscillations combined with the incapability of the Power System Stabilizers (PSSs) to provide the adequate damping for these oscillations [8,9]. All these factors would much more likely create a heavy power flow conditions in interconnected power systems with the consequent uprising of unstable inter area oscillations. Therefore, stabilizing of unstable inter-area oscillations has been a matter of great importance in the power industry due to their serious consequences on the power network [10]. Moreover, even the presence of the poorly damped inter-area oscillations imposes limits on the power transfer capacity of a transmission corridor and jeopardizes the intact operation of interconnected power systems by being one of the main reasons behind many worldwide blackouts.

Utilization of dynamic braking resistor is one of the multiple presently conceivable stabilization methods for inter-area oscillations. Dynamic braking resistor was firstly recommended by the European Network of Transmission System Operators-for-Electricity-Continental Europe Synchronous Area (ENTSO-E-CESA) working committee to the Turkish Transmission System Operator, as precautionary countermeasure, in anticipation of the poorly damped 0.15 Hz inter-area oscillation mode which was a collateral result for the synchronous interconnection between the Turkish power system and the ENTSO-E-CESA in 2009 [11]. There are plenty of researches in the literature regarding the implementation of the dynamic braking resistor for transient stability augmentation, and steam turbine-generator shaft torsional oscillations alleviation using mostly local control signal such as generator speed deviation [12,13]. With regard to the power system point of view, the conceptual principal of the dynamic braking resistor is simply to add an extra dummy load to absorb any excess energy developed during the system dynamic disturbances and remove it elsewhere.

The stabilization approach suggested herein inspired from the conclusions presented in [14]. The authors presented single Thyristor Controlled Braking Resistor (TCBR) unit for stabilization of inter-area oscillations in Kundur's two-area test system and the energization signal for the brake was the speed of equivalent one-machine infinite bus (OMIB) system without considering any AI-based controller. Also, the authors presented the response of equivalent OMIB speed to highlight the stabilization capability of the single installed TCBR. This study will explore dual fuzzy logic controllers (FLCs), one for each area, to orchestrate a coordinated switching strategy for dual TCBRs for stabilizing inter-area power oscillations in Kundur's two-area test system. This study will introduce the responses of inter-area active and reactive power to demonstrate the stabilization capability of the proposed scheme. This work will implement the relative kinetic energy deviation for each area as control signal for the FLC.

In summary, unstable inter-area oscillations have been long recognized as the main culprit for many worldwide blackout events. The unstable nature of these oscillations comes mainly from stressed interconnecting tie-lines. The main reasons for this stress are deregulation, unceasing worldwide interconnection projects, and transferring bulk power transactions over long distances. Therefore, stabilization of unstable inter area oscillations, in a cost-effective manner, will prevent many blackout events. In this study,

stabilization of unstable inter area oscillations is achieved by implementation of dual dynamic braking resistors.

The rest of this paper is organized as follows. In section 2, a brief description of the system under study is presented. In section 3, the idea of utilizing the FLC to control the proposed scheme is introduced. In section 4, MATLAB™/Simulink comparative time domain simulation results are depicted with comments. In section 5, the main conclusions of the research are presented. Finally, the list of references used in this work is presented.

2. TEST SYSTEM DESCRIPTION

To scrutinize the effectiveness of the suggested stabilization regime in this paper, the well-known Kundur Benchmark test system is considered. The two-area test system has four machines and the single-line diagram of the system is depicted in Figure 1. It is a hypothetical interconnected power system with realistic parameters, and it is widely employed for studying power system oscillations. This model was first engineered by Ontario Hydro for the sake of a survey report commissioned by the Canadian Electrical Association (CEA) to study this vital power system problem.

The base test system is composed of two similar areas (active networks) connected via two parallel 230 kV tie-lines with a relatively long transmission distance of 220 Km which makes the transmission link relatively weak especially with aggregate power transfer. Each area possesses two fully identical round rotor (60 Hz) synchronous generators rated 20 kV/900 MVA and the only parameters discrepancy is the inertia constant (H) which equals 6.5 seconds for each machine in area 1, and 6.175 seconds for each machine in area 2, respectively.

All the generators are driven by the same type of prime mover which is supposedly steam turbine in this work. For the sake of brevity, the parameters and the dynamic data for the test system are available in. Three low-frequency electromechanical modes of oscillation are existent in the system, two local modes, one in each area, and one inter-area mode, and they are often stimulated simultaneously. As similar to the work found in [4], the distribution of loads and generated powers causes an electric power transaction of 413 MW to be exported from generation-rich area 1 to area 2 which is happened to be suffering from a shortage in the generation, as indicated from the direction of the arrow shown in Figure 1.

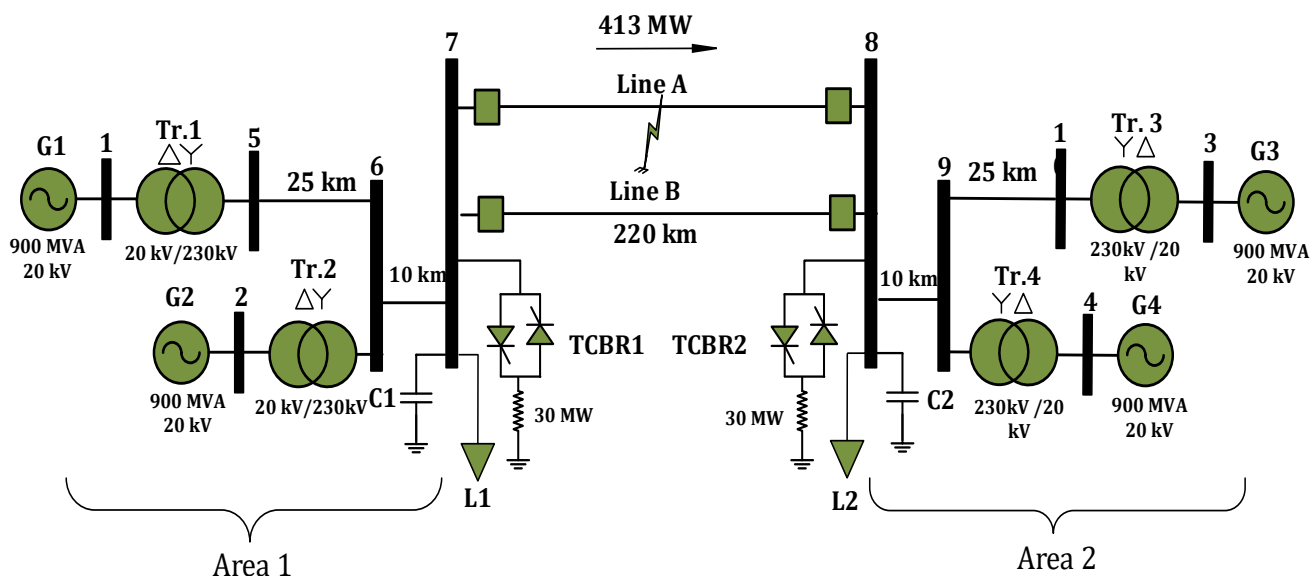


Figure 1: Single-line diagram of four-machine two-area test system with double 30 MW TCBRs

Two 30 MW TCBRs are installed at both ends of the interconnecting transmission link at bus 7 and at bus 8, i.e. one TCBR for each area. Each TCBR is controlled via separately dedicated FLC to orchestrate the dynamic braking interventions for the test system. Both areas of the test system, as expected, are susceptible to undergo inter-area oscillation for the different grid disturbances. Detailed depictions of each TCBR are shown in Figure 2.

Local control signals are not the only possible control signal that could be utilized as an energization signal for the dynamic braking resistor but, global control signals such as total kinetic energy deviation (TKED) and the time derivative of the TKED could also be employed [15]. In this work, the relative kinetic energy deviation between the two areas is used as input energization signal to each FLC.

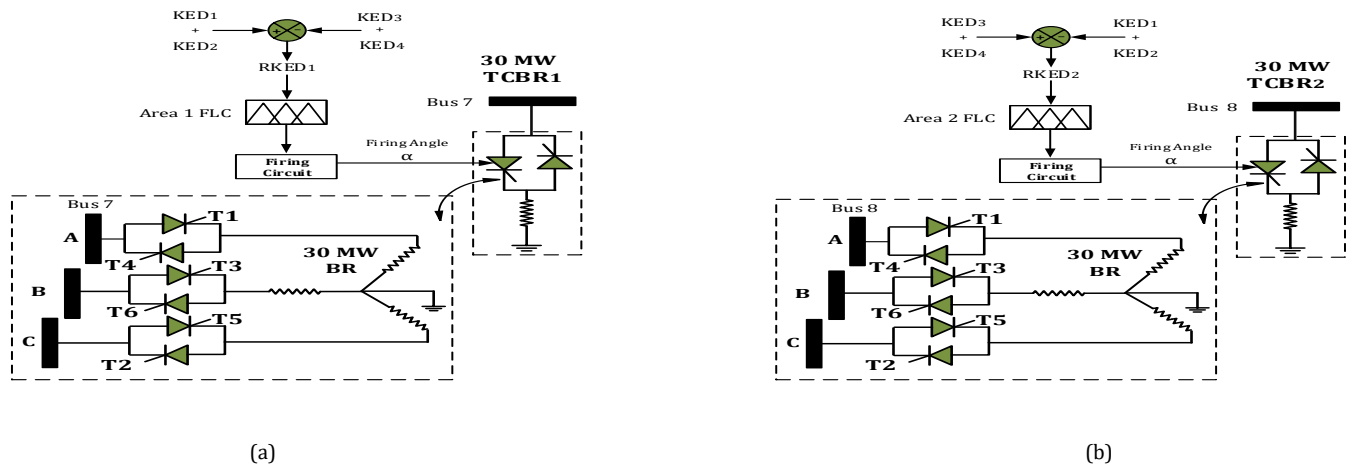


Figure 2: Detailed depictions for each of the dual TCBR with the FLC and the input control signal (a) Detail of Area 1 TCBR installed at bus 7, (b) Detail of Area 2 TCBR installed at bus 8

To obtain the relative kinetic energy deviation for each area, the kinetic energy deviation for each machine (KED_i) in joule is calculated as follows, $KED_i = (\text{machine kinetic energy at transient state}) - (\text{machine kinetic energy at steady state})$. Throughout this section, $i=1, 2, 3,$ and 4 denoting the machine number in the test system.

$$KED_i = \frac{1}{2} [J_i \omega_i^2] - \frac{1}{2} [J_i \omega_o^2] \quad \text{joule} \quad (1)$$

Where J_i denotes the rotor moment of inertia in Kg. m² for machine i , ω_i is machine angular speed in (mechanical rad/s) and ω_o is machine synchronous angular speed in (mechanical rad /s). Then the relative kinetic energy deviation for area 1 ($RKED_1$) = total kinetic energy deviation for area 1 - total kinetic energy deviation for area 2.

$$\begin{aligned} RKED_1 &= \left[\left(\frac{1}{2} J_1 \omega_1^2 - \frac{1}{2} J_1 \omega_o^2 \right) + \left(\frac{1}{2} J_2 \omega_2^2 - \frac{1}{2} J_2 \omega_o^2 \right) \right] \\ &- \left[\left(\frac{1}{2} J_3 \omega_3^2 - \frac{1}{2} J_3 \omega_o^2 \right) \right. \\ &+ \left. \left(\frac{1}{2} J_4 \omega_4^2 - \frac{1}{2} J_4 \omega_o^2 \right) \right] \quad \text{joule} \quad (2) \end{aligned}$$

And, the relative kinetic energy deviation for area 2 ($RKED_2$) = total kinetic energy deviation for area 2 - total kinetic energy deviation for area 1.

$$\begin{aligned} RKED_2 &= \left[\left(\frac{1}{2} J_3 \omega_3^2 - \frac{1}{2} J_3 \omega_o^2 \right) + \left(\frac{1}{2} J_4 \omega_4^2 - \frac{1}{2} J_4 \omega_o^2 \right) \right] \\ &- \left[\left(\frac{1}{2} J_1 \omega_1^2 - \frac{1}{2} J_1 \omega_o^2 \right) \right. \\ &+ \left. \left(\frac{1}{2} J_2 \omega_2^2 - \frac{1}{2} J_2 \omega_o^2 \right) \right] \quad \text{joule} \quad (3) \end{aligned}$$

An elaborate TCBR model is built in MATLAB[™]/Simulink environment using three antiparallel pairs of high-power thyristors to compose three-phase AC voltage controller through which three-phase star-connected 30 MW linear resistor bank is connected to the high voltage busses number 7 and 8 as shown schematically in Figure 2. The proposed strategy in this paper relied on the hypothetical post-existence of the communication infrastructure needed for the control signal acquisition and transmission from the different power plants in the test system to the centralized FLC dedicated for each area. The power system simulation is implemented in SimPower[®] of MATLAB[™]/Simulink which is possible to find the complete system as a demo [16].

3. DESIGN OF FUZZY LOGIC CONTROLLER

Over the years, fuzzy-logic control has been suggested for a considerable number of multidisciplinary power system problems [17]. Fuzzy logic is dissimilar from the crispy counterpart in Boolean theory which uses only two logical levels (0 or 1) in that it uses unlimited logical levels (from 0 to 1) to resolve issues that have uncertainties or ambiguous situations. FLCs

are confirmed to be more robust and their performances possess a lesser sensitivity to the parametric variations than the traditional controllers [12]. FLC is a nonlinear controller based on the use of expert knowledge, alternatively speaking it is a rule-based intelligent system. A set of fuzzy rules commonly characterized by "IF-THEN" statements which exemplify a control decision-making mechanism for regularizing the fuzzy output for the different system stimuli [18].

The basic configuration of FLC is composed of the following four incipient stages: fuzzification, knowledge base, inference engine, and defuzzification. In the fuzzification stage, the input crisp values are mapped into fuzzy variables using normalized membership functions and occasionally input gains (weighting factors). The fuzzy-logic inference engine concludes the convenient control action based on the obtainable rule base and there are two main types Takagi-Sugeno (TS), and Mamdani. The fuzzy control action is converted to proper crisp value through the defuzzification process using normalized membership functions and occasionally output gains (output weighting factors). TS inference type is more efficient than the Mamdani inference type for dynamic systems with rapid variable dynamics. TS type also works satisfactorily with linear; adaptive and optimization techniques and it is very appropriate for mathematical analysis. Therefore, TS inference mechanism is utilized in the simulation study.

Gaussian and Sigmoid membership functions are selected to represent the input control variable of the fuzzy controller (i.e. RKED in per unit system, p.u.-s). The input membership functions for the system are shown in Figure 3 in which three linguistic variables, namely, NB (Negative Big), Z (Zero), and PB (Positive Big), are defining the fuzziness of the controller input. The parameters of the membership functions utilized in this study are fixed throughout the simulation study for all case studies and determined by trial-and-error approach. The output type is constant having either 0 or 1 values (0 for both Z and NB, 1 for PB). Where 0 indicates that the TCBR should be fully OFF and 1 indicates that the TCBR should be fully ON.

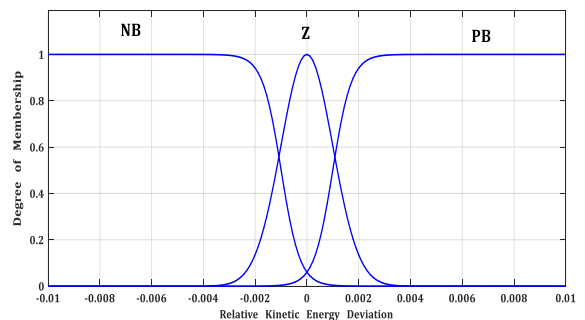


Figure 3: Membership function of RKED [p.u.-s]

The proposed control scheme is direct and simple since it has only three control rules where the TCBR is inserted if the RKED exceeds a certain value (i.e. the area has excess kinetic energy) and removed elsewhere (steady-state or the area has lack of the kinetic energy). There are three premise membership functions in Figure 3 and the conclusions are constants so the fuzzy control rules are as follows, If the input (RKED) is NB then the output is 0, If the input (RKED) is Z then the output is 0, and If

the input (RKED) is PB then the output is 1. Then the firing angle circuit will provide the necessary firing angle, α , pulses for the thyristors (for fuzzy output 0 then $\alpha=180^\circ$, and for fuzzy output 1 then $\alpha=0^\circ$). In the next section, nonlinear time domain simulations are performed to highlight the capability of fuzzy controlled TCBRs to effectively stabilize inter-area power oscillations through ON-OFF (bang-bang) fuzzy-based control.

4. TIME DOMAIN SIMULATION RESULTS AND DISCUSSION

The assessment of fuzzy-based dynamic braking performance is accomplished by considering three case studies including small, mild, and severe disturbances which will demonstrate the effectiveness and the authenticity of the proposed scheme. All the following case studies are conducted considering a power flow situation in which active power of 413 MW is transferred from area 1 (the exporting area) to area 2 (the importing area).

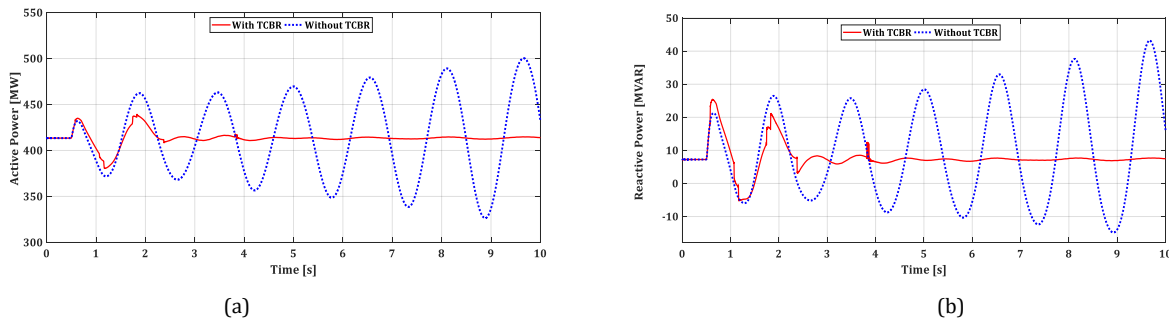


Figure 4: Power flow responses to the small disturbance with and without the dynamic brake, (a) Inter-area active power flow, (b) Inter-area reactive power flow

The unstable oscillatory nature of the inter-area mode of oscillation can be clearly seen from the outline of Figure 4. As it is obviously noticed, without the proposed scheme, the amplitudes of the power swings are periodically increasing. Inevitably, the protection system shall be forced to take tripping action of the system elements and then the whole power system collapses. With the proposed scheme, the system oscillatory behavior is mitigated after nearly 2 seconds after the disturbance inception. A simple

understanding of the TCBR functioning can be obtained by analyzing the behavior of the dissipated power in the TCBR together with the insertion control signal. Thus, Figure 5 shows the responses of the RKED and three-phase dissipated power in TCBR for both areas with and without the proposed scheme.

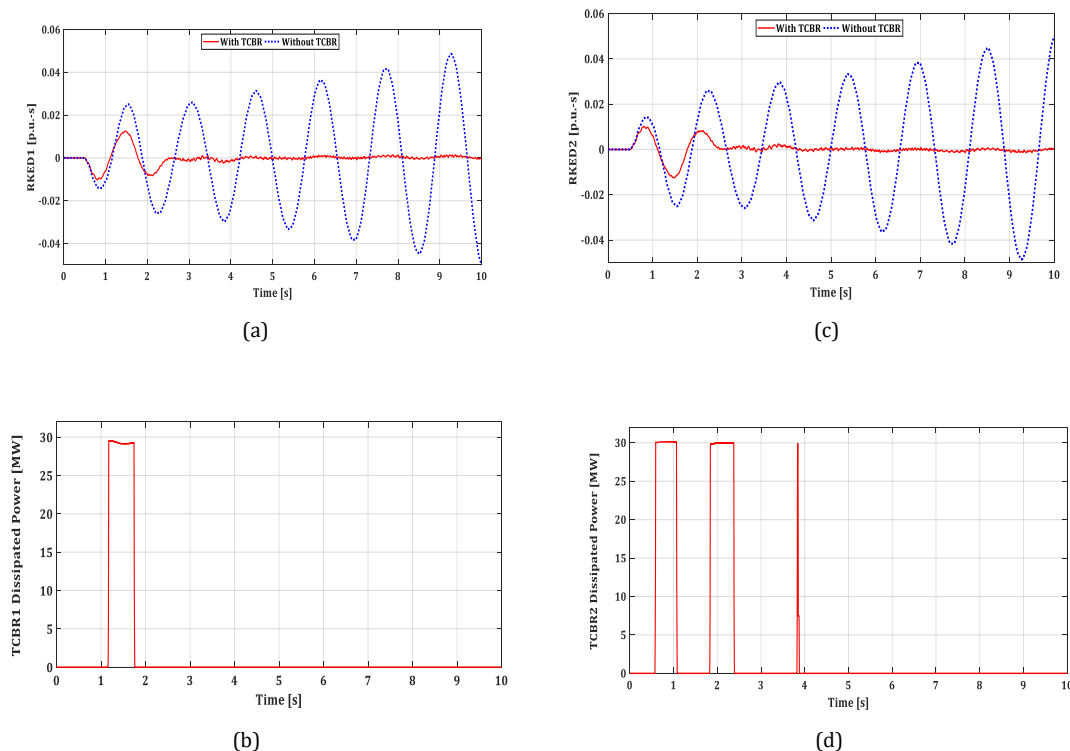


Figure 5: Case (1) RKED and TCBR power responses due to small step change in the reference voltage of machine (1) (a) RKED for area 1, (b) TCBR1 dissipated power, (c) RKED for area 2, and (d) TCBR2 dissipated power

Referring to Figure 5, in the steady state of the power system, the dissipation through each TCBR is intuitively zero. Since the amount of dissipated power through TCBR for each area depends on the excess

kinetic energy deviation in that area therefore, it is observed the power dissipation becomes zero after 1.756 seconds for TCBR1 and after 3.874 seconds for TCBR2 and they still so to the end of the simulation time. This

fact indicates that the system relative kinetic energy deviations become virtually zero due to the coordinated fuzzy-based operation of the dual TCBRs.

4.2 Case Study 2— Inadvertent Tripping of Tie-Line (A)

Referring to Figure 1, the interconnecting tie-line (A) is inadvertently tripped by simultaneous operation of the two-circuit breakers located at

the terminals of the tie-line due to relaying system maloperation (i.e. without any system fault) at $t = 0.5$ second from the simulation time and no high-speed reclosure (HSR) is considered. Plots for the active power and reactive power exported from area 1 to area 2 (as recorded on bus 7) with and without the fuzzy-based dynamic braking interventions are shown in Figure 6.

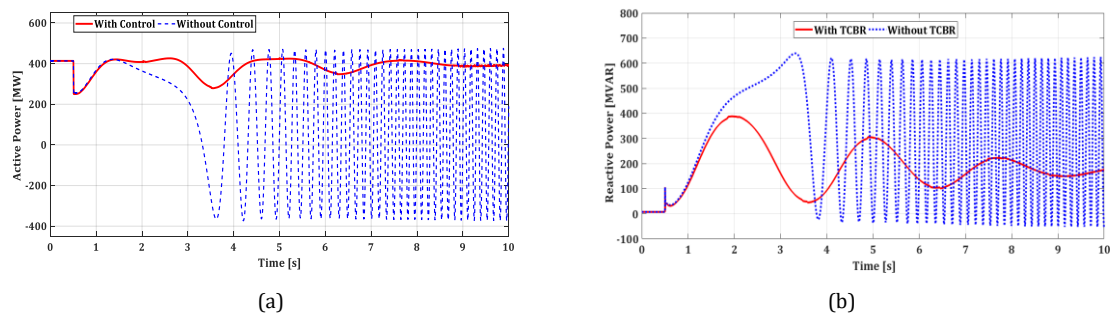


Figure 6: Power flow responses due to tripping of tie-line (A) with and without dynamic brake

(a) Inter-area active power flow, (b) Inter-area reactive power flow

The system performance comparison plot depicted in Figure 6 shows clearly that the system will lose its stability without the dynamic braking interventions after about 3 seconds from the disturbance initiation. With the fuzzy-based dynamic braking interventions, the system will be

stabilized, and the power oscillations are mitigated as the simulation time proceeds. Then, in Figure 7 it is shown the response of the RKED and three-phase dissipated power in the TCBR for each area with and without the proposed scheme.

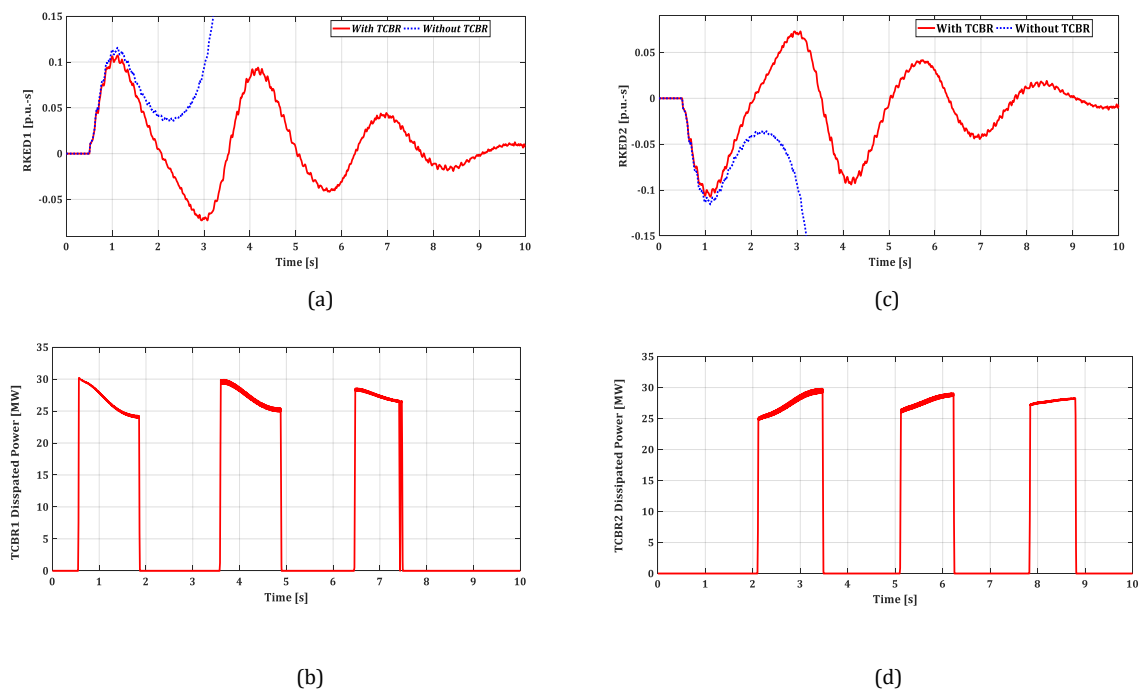


Figure 7: Case (2) RKED and TCBR dissipated power responses (a) RKED for area 1, (b) TCBR1 dissipated power, (c) RKED for area 2, and (d) TCBR2 dissipated power

As it is obvious from the response of the RKED without the proposed scheme that the machines in area 1 gain considerably huge kinetic energy which will be stored in their rotors and causes the machines in that area to accelerate astronomically and finally lose their synchronism. In contrast, the machines in area 2 lose their kinetic energy very rapidly which causes the machines in that area to decelerate considerably and finally lose their synchronism. The operation of the dynamic braking has stymied the kinetic energy deviation of the system from excessive changes with the consequent stability loss.

4.3 Case Study 3— Unsuccessful Reclosure of Three-Phase to Ground Fault at the Middle of Tie-Line (A)

In this study, the tie-line power flow is analyzed when the system is subjected to three-phase permanent bolted short circuit (3LG) at tie-line (A), connecting bus 7 to bus 8 as shown in Figure 1, at the middle of the line at time $t = 0.5$ second and HSR of the circuit breakers is considered in this case which will be intuitively unsuccessful. The case scenario calls for clearing the fault in 3 cycles (0.05 second) from the disturbance initiation by the simultaneous breaking action of the two circuit breakers located at the terminals of the tie-line (A). Then the two circuit breakers reclose simultaneously after 30 cycles (0.5 second) later and then finally reclear the fault again after another 3 cycles (0.05 second) and stay open with no further reclosure attempts for the end of the simulation time. The two curves are shown in Figure 8 highlight the comparison of the active and reactive power transfer of the system due to this severe disturbance.

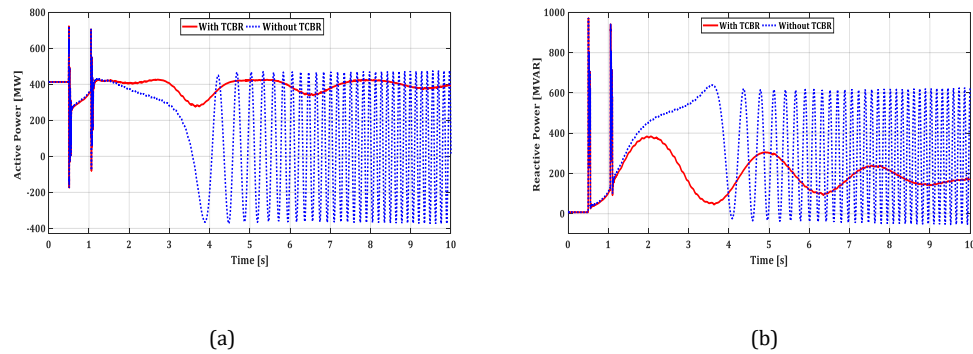


Figure 8: Power flow responses due to the unsuccessful reclosure of tie-line (A) with and without dynamic brake, (a) Inter-area active power flow, (b) Inter-area reactive power flow

It is evident from the time domain simulation results that, the system loses its stability after nearly 3 seconds of the simulation time. But, due to the operation of the dynamic braking resistor, the system will be stabilized and the power oscillations are mitigated as the simulation time proceeds.

The responses of the RKED and three-phase dissipated power in each TCBR with and without the proposed scheme are depicted in the series of curves shown in Figure 9.

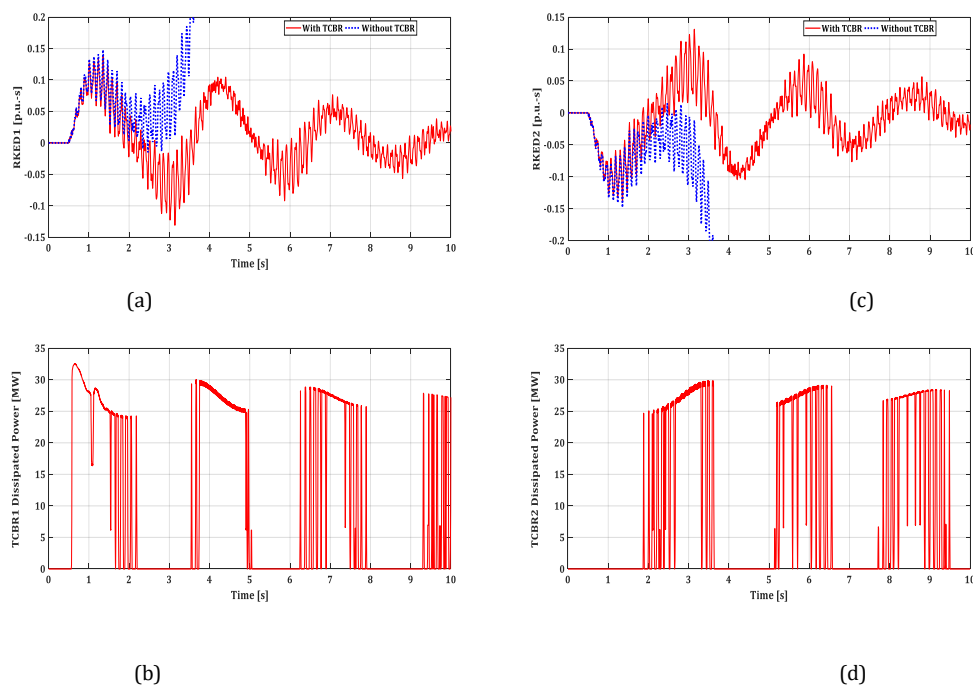


Figure 9: Case (3) RKED and TCBR dissipated power responses(a) RKED for area 1, (b) TCBR1 dissipated power, (c) RKED for area 2, and (d) TCBR2 dissipated power

Finally, as depicted in Figure 9, the system loses its synchronism without the proposed scheme after about 3 seconds of the simulation time. Due to the presence of the fuzzy-based TCBR operations, the kinetic energy deviation of the system will be stymied allowing the system to maintain synchronism.

5. CONCLUSIONS

This paper proposed fuzzy-based switching strategy for the coordinated energization of dual TCBRs in weakly interconnected Kundur Benchmark two-area test system to stabilize unstable inter-area oscillations manifested due to transferring heavy power flow conditions. The effectiveness of the proposed stabilization scheme is examined by taking into consideration three case studies with various degrees of severity. By analyzing the performance repercussions raised due to the considered perturbations, without the employment of the proposed scheme, the unstable nature of the power flow and the RKED responses can be obviously observed. With the employment of the proposed scheme, the system oscillatory behavior is stabilized in an acceptable manner. The performed comparative non-linear time-domain simulation results emphasize the great potential of dynamic braking resistor, as a cost-effective stabilization candidate, in stabilizing inter-area oscillations according to the considered disturbances. This work concludes by emphasizing the great importance of the proposed scheme in reducing the

vulnerability of interconnected power systems to cascading element outages by neutralizing the threats of unstable inter-area oscillations.

REFERENCES

- [1] Ping, J. 2018. Stochastic Dynamics of Power Systems, Springer, Singapore.
- [2] Leonard, L.G. 2012. Power System Stability and Control, third ed., Taylor & Francis, United States.
- [3] Zeng, B., Ouyang, S.J., Zhang, J.H., Shi, H., Wu, G., Zeng, M. 2015. An Analysis of Previous Blackouts in The World: Lessons for China's Power Industry, Renewable and Sustainable Energy Reviews, 42:1151–1163 DOI: 10.1016/j.rser.2014.10.069
- [4] Hadjikypris, M. 2015. Supervisory Control Scheme for FACTS and HVDC Based Damping of Inter-Area Power Oscillations in Hybrid AC-DC Power Systems, Ph.D. Thesis, University of Manchester, United Kingdom.
- [5] Wang, H.F., Du, W.J. 2016. Analysis and Damping Control of Power System Low-frequency Oscillations, Springer, United States.
- [6] Chellam, S., Kalyani, S. 2016. Power Flow Tracing-Based Transmission Congestion Pricing in Deregulated Power Markets, International Journal of Electrical Power & Energy Systems, 83, 570–584 DOI: 10.1016/j.ijepes.2016.03.049

- [7] Khan, M.T., Siddiqui, A.S. 2014. Congestion Management in Deregulated Power System Using FACTS Device, *International Journal of System Assurance Engineering and Management*, 8, 1-7, DOI: 10.1007/s13198-014-0258-x
- [8] Ulf Häger, U., Christian Rehtanz, C., Nikolai Voropai, N. 2014. *Monitoring, Control and Protection of Interconnected Power Systems*, Springer, Germany.
- [9] Li, Y., Yang, D.C., Liu, F., Cao, Y.J., Rehtanz, C. 2016. *Interconnected Power Systems: Wide-Area Dynamic Monitoring and Control Applications*, Springer, Germany.
- [10] You, S., Kou, G., Liu, Y., Zhang, X., Cui, Y., Till, M.J., Yao, W., Liu, Y. 2017. Impact of High PV Penetration on the Inter-Area Oscillations in the U.S. Eastern Interconnection, *IEEE Access*, 5, 1-6 DOI: 10.1109/access.2017.2682260
- [11] Ahmed, M.F., Ebrahim, M.A., EL-Hadidy, M.A., Mansour, W.M. 2016. Torsional Oscillations Mitigation via Novel Fuzzy Control Based Braking Resistor Model, *International Electrical Engineering Journal (IEEJ)*, 7, 2173 - 2181.
- [12] Ahmed, M.F., Ebrahim, M.A., EL-Hadidy, M.A., Mansour, W.M. 2018. Torsional Oscillations Mitigation for Interconnected Power System Via Novel Fuzzy Control Based Braking Resistor Model, *International Council on Large Electric Systems (CIGRE)*, France, 1 - 9
- [13] Tor, O.B., Gencoglu, C., Yilmaz, O., Cebeci, E., Guven, A.N. 2010. Damping Measures against Prospective Oscillations between Turkish Grid and ENTSO-E System, *Proceeding of IEEE International Conference on Power System Technology (POWERCON)*, China, 1-7, DOI: 10.1109/POWERCON.2010.5666448
- [14] Huseinbasic, E., Kuzle, I., Tomisa, T. 2009. Inter-Area Oscillations Damping using Dynamic Braking and Phasor Measurements, *Proceeding of IEEE/PES Power Systems Conference and Exposition (PSCE)*, USA, 1 - 6, DOI: 10.1109/PSCE.2009.4840068
- [15] Ahmed, M.F., Mandor, M.A., EL-Hadidy, M.A., Bendary, F.M. 2019. Inter-Area Power Oscillations Mitigation for Electrical Systems Via Novel Fuzzy Control Based Braking Resistor, *Proceedings of CIRED Conference*, Paper no. 134, Spain, 1 - 5
- [16] Kamwa, Comparison of three Power System Stabilizer (PSS) using Kundur's Four-Machine Two-Area Test System, *MATLAB™ Demo*
- [17] Altas, I.H. 2017. *Fuzzy Logic Control in Energy Systems with Design Applications*. Institution of Engineering & Technology, United Kingdom.
- [18] Romulo Antão, R. 2017. *Type-2 Fuzzy Logic Uncertain Systems' Modelling and Control*, Springer, Singapore

